SCIENTIFIC REPORTS
nature research

OPEN

A new nickel-based co-crystal complex electrocatalyst amplified by NiO dope Pt nanostructure hybrid; a highly sensitive approach for determination of cysteamine in the presence of serotonin

Hassan Karimi-Maleh[1,2,3]✉, Fatemeh Karimi[4,5]✉, Yasin Orooji[6,7], Ghobad Mansouri[8], Amir Razmjou[9,10,11], Aysenur Aygun[12] & Fatih Sen[12]✉

A highly sensitive electrocatalytic sensor was designed and fabricated by the incorporation of NiO dope Pt nanostructure hybrid (NiO–Pt–H) as conductive mediator, bis (1,10 phenanthroline) (1,10-phenanthroline-5,6-dione) nickel(II) hexafluorophosphate (B,1,10,P,1,10, PDNiPF6), and electrocatalyst into carbon paste electrode (CPE) matrix for the determination of cysteamine. The NiO–Pt–H was synthesized by one-pot synthesis strategy and characterized by XRD, elemental mapping analysis (MAP), and FESEM methods. The characterization data, which confirmed good purity and spherical shape with a diameter of ~ 30.64 nm for the synthesized NiO–Pt–H. NiO–Pt–H/B,1,10, P,1,10, PDNiPF6/CPE, showed an excellent catalytic activity and was used as a powerful tool for the determination of cysteamine in the presence of serotonin. The NiO–Pt–H/B,1,10, P,1,10, PDNiPF6/CPE was able to solve the overlap problem of the two drug signals and was used for the determination of cysteamine and serotonin in concentration ranges of 0.003–200 µM and 0.5–260 µM with detection limits of 0.5 nM and 0.1 µM, using square wave voltammetric method, respectively. The NiO–Pt–H/B,1,10,P,1,10,PDNiPF6/CPE showed a high-performance ability for the determination of cysteamine and serotonin in the drug and pharmaceutical serum samples with the recovery data of 98.1–103.06%.

Cysteamine is a simple aminothiol with a variety of medicinal applications used to treat various diseases such as cystinosis and hypothyroidism[1]. Cysteamine is prescribed as a radiation-protective agent drug to treat radiation

[1]School of Resources and Environment, University of Electronic Science and Technology of China, Xiyuan Ave, P.O. Box 611731, Chengdu, People's Republic of China. [2]Department of Chemical Engineering, Laboratory of Nanotechnology, Quchan University of Technology, Quchan, Islamic Republic of Iran. [3]Department of Chemical Sciences, University of Johannesburg, Doornfontein Campus, P.O. Box 17011, Johannesburg 2028, South Africa. [4]Nanostructure Based Biosensors Research Group, Ton Duc Thang University, Ho Chi Minh City, Vietnam. [5]Faculty of Applied Sciences, Ton Duc Thang University, Ho Chi Minh City, Vietnam. [6]Co-Innovation Center of Efficient Processing and Utilization of Forest Resources, Nanjing Forestry University, Nanjing 210037, China. [7]College of Materials Science and Engineering, Nanjing Forestry University, Nanjing 210037, People's Republic of China. [8]Department of Chemistry, Payame Noor University, P.O. Box 19395-3697, Tehran, Iran. [9]Department of Biotechnology, Faculty of Biological Science and Technology, University of Isfahan, 81746-73441 Isfahan, Iran. [10]School of Chemical Science and Engineering, UNESCO Centre for Membrane Science and Technology, University of New South Wales, Sydney 2052, Australia. [11]Department of Engineering, Macquarie University, Sydney, NSW 2109, Australia. [12]Sen Research Group, Biochemistry Department, Faculty of Arts and Science, Dumlupınar University, Evliya Çelebi Campus, 43100 Kütahya, Turkey. ✉email: hassan@uestc.edu.cn; fatemeh.karimi@tdtu.edu.vn; fatihsen1980@gmail.com

sickness[2]. Overdose of cysteamine brings about many side effects such as dizziness, rash, skin odor, headache, and tiredness. Therefore, the analysis of cysteamine should be monitored for administrated patients. On the other hand, taking cysteamine is effective in the serotonin neurotransmission level in body[3]. Also, the use of cysteamine in the treatment of patients can change tissue serotonin in duodenal ulceration[4]. Therefore, the simultaneous measurement of these two compounds is pivotal in the patients treated with cysteamine. Due to the important analysis of these compounds, many researchers focused on the fabrication of analytical sensors for their determination in biological and clinical samples[5–9]. Although there have been no reports on the simultaneous measurement of cysteamine and serotonin, various analytical methods such as chromatography, spectroscopy, and electrochemical sensors have been separately reported for each of these compounds[8,10–13]. Due to simple operations and low-cost analysis systems, electrochemical sensors have been widely used for the analysis of pharmaceutical and biological compounds[14–21]. Near over-potential oxidation of cysteamine and serotonin on the surface of a bare electrode is one of the most important problems in the simultaneous analysis of cysteamine and serotonin, using electrochemical methods[22]. Therefore, the application of electro-catalyst is necessary for resolving this issue in the simultaneous analysis[23–30]. EC/ electrochemical mechanism is a suitable strategy for the determination of two analytes with near over-potential in electrochemical analysis systems[31–37]. The interaction of one analyte with a suitable electrocatalyst and remaining of another analyte at its potential is a very interesting strategy based on electrocatalytic systems in the simultaneous analysis[37–41]. Selecting a suitable catalyst with high selectivity is one of the most important steps in the design of electrocatalytic sensors[42–46]. According to previous reports, inorganic complexes, especially complexes with nickel central atom can be used as a suitable electrocatalyst in the analysis of important pharmaceutical and biological constituents[47–52]. Although nanomaterials such as carbon nanotubes and graphene with high-conductivity have been proposed for the preparation of electrochemical sensors, their high cost, hard synthesis methods, and high capacitive charging current are some of the most important criteria for their use in electrochemical sensors[53–61]. Accordingly, the use of metal oxides has been used as a suitable alternative to this category of materials[62–66]. Recent research suggests that modifying metal oxides with metal nanoparticles such as platinum could increase the electrical conductivity of the sensors and create the right conditions for the design of high-sensitivity sensors[67].

Therefore, in this study, we fabricated NiO–Pt–H/B,1,10,P,1,10,PDNiPF6/CPE as a first and highly sensitive electroanalytical sensor for simultaneous determination of cysteamine and serotonin. The NiO–Pt–H/B,1,10,P,1,10,PDNiPF6/CPE was successfully used for the determination of cysteamine and serotonin in real samples.

Experiment

Instruments and materials. Electrochemical signals were recorded by Potentiostat/Galvanostat Electrochemical Instrument PGSTAT-302N (Netherlands). The Field Emission SEM machine model Mira 3-XMU was used for morphological and EDS analysis of NiO dope Pt nanostructure hybrid. The structural analysis of NiO dope Pt nanostructure hybrid was characterized by XRD machine model X'Pert Pro. The Ag/AgCl/KClsat and electrochemical cell were purchased from Azar Electrode Company.

Cysteamine hydrochloride and serotonin hydrochloride were purchased from Sigma-Aldrich Company. The 0.01 M stock solution of cysteamine hydrochloride and serotonin hydrochloride was prepared by dissolving 0.113 g and 0.212 g compounds in 100 mL phosphate buffer solution (PBS) pH 7.0.

Nickel nitrate hexahydrate, sodium hydroxide, and platinum (II) chloride were purchased from Merck Company and used for one-pot synthesis of NiO dope Pt nanostructure hybrid. Phosphoric acid was purchased from Acros Company and used for the preparation of PBS.

Synthesis of NiO dope Pt nanostructure hybrid. The 100-mL solution containing 16 mg platinum (II) chloride and 0.5 M nickel nitrate hexahydrate were stirred for 30 min at room temperature. The 100-mL sodium hydroxide 1.0 M was added to the previous solution over a 1.5 h period. The green precipitated sample was filtered and then dried at 15 h at 100 °C. The green powder was calcined at 400° C in a furnace for 3 h.

Preparation of NiO–Pt–H/B,1,10,P,1,10,PDNiPF6/CPE. The NiO–Pt–H/B,1,10,P,1,10,PDNiPF6/CPE was designed and made by using slurry composed of 0.95 gr of graphite powder 0.04 g + NiO–Pt–H and 0.05 g of B,1,10,P,1,10,PDNiPF6 using 13 drops of paraffin oil as binders into mortar and pestle in the presence of 10 mL ethanol. After evaporation of the ethanol solvent, the mixture was hand-mixed for 90 min to obtain a homogeneous paste.

Preparation of real sample. Cysteamine capsules (150 mg) were purchased from a local pharmacy and after opening 10 capsules, the powder was dissolved into a 100-mL solution containing ethanol/PBS 1:1 and stirred for 1 h. Dilution was performed using phosphate buffer solution.

Recommend procedure. Electrochemical behavior of cysteamine was investigated by recording cyclic voltammograms of 500 µM cysteamine on the surface of NiO–Pt–H/B,1,10,P,1,10,PDNiPF6/CPE, B,1,10,P,1,10,PDNiPF6/CPE, NiO–Pt–H/CPE and CPE at pH 7.0 and scan rate 10 mV/s. Then, the recorded cyclic voltammograms were compared together for the investigation catalytic effect of the fabricated sensors.

Interference study was investigated by recording square wave voltammogram (SWV) of 20.0 µM cysteamine on the surface of NiO–Pt–H/B,1,10,P,1,10,PDNiPF6/CPE. The 20.0 µM in the electrochemical cell containing 10 mL buffer solution was equal to 2.2×10^{-6} g of cysteamine in solution. In the next step and after the addition of interference with a maximum acceptable value of 1,000 fold (w/w) into an electrochemical cell, the signal of

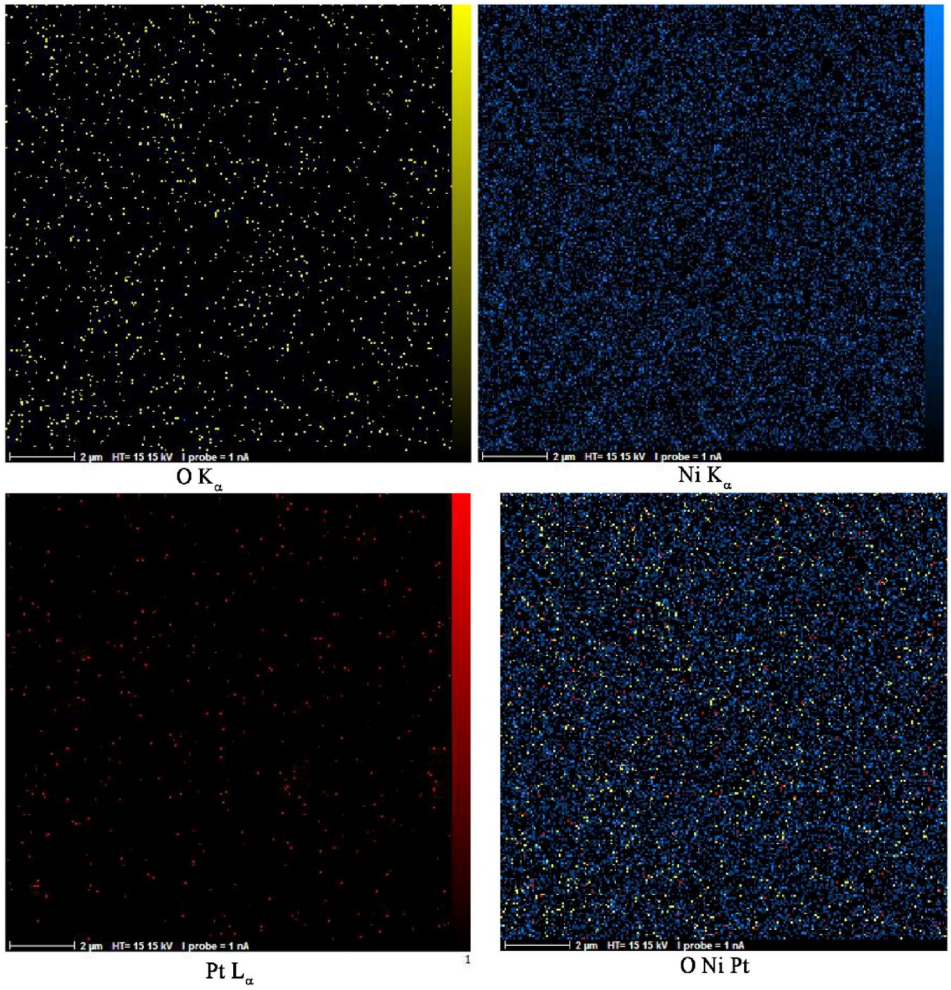

Figure 1. MAP analysis data for synthesized NiO dope Pt nanostructure hybrid.

the solution containing cysteamine and interference was recorded. The 5% error in current was acceptable and showed that interference did not have a significant effect on the analysis signal.

Stability of NiO–Pt–H/B,1,10,P,1,10,PDNiPF6/CPE as an electroanalytical sensor for determination of cysteamine was investigated by recording SWV of 100.0 µM cysteamine over a course of 60 days on the surface of the fabricated sensor. The drug signal was recorded every ten days and the current obtained was compared with the initial current of the drug.

Results and discussion

Characterization of NiO–Pt–H. The purity and particle distribution of NiO–Pt–H were characterized by MAP analysis. The results are presented in Fig. 1, showing good distribution and purity of the synthesized NiO–Pt–H. In addition, the FESEM figure showed a spherical shape for synthesized NiO–Pt–H with good distribution in nanoparticle sizes (Fig. 2A). Furthermore, the XRD pattern of NiO–Pt–H showed planes with miller indexes of (1 1 1), (2 0 0), (2 2 0), (3 1 1), and (2 2 2) relative to NiO particle with a code No. 04-0835. On the other hand, due to the low concentration of Pt in a synthesized nano-hybrid, the Pt planes could not be detected in XRD pattern (Fig. 2B).

Electrocatalytic determination of cysteamine using NiO–Pt–H/B,1,10,P,1,10,PDNiPF6/CPE. The cyclic voltammograms NiO–Pt–H/B,1,10,P,1,10,PDNiPF6/CPE (Fig. 3, curve a) was recorded in the phosphate buffer solution (pH 7.0). Recording voltammogram showed a redox signal with quasi behavior ($\Delta E = 73$ mV) relative to Ni^{2+}/Ni^{3+} in the absence of cysteamine. After the addition of 500 µM cysteamine on the surface of NiO–Pt–H/B,1,10,P,1,10,PDNiPF6/CPE, the oxidation current of B,1,10,P,1,10,PDNiPF6 increased and the reduction signal of mediator was removed ($E_{Oxidation} \sim 120$ mV). This phenomenon exhibits a kind of electrocatalytic behavior between the intermediate (B,1,10,P,1,10,PDNiPF6 in this case) and the cysteamine (see Scheme 1). On the other hand, on the surface of B,1,10,P,1,10,PDNiPF6/CPE (Fig. 3, curve c), the same electrocatalytic behavior with a weaker signal was observed, which can be attributed to the role of nanoparticles on

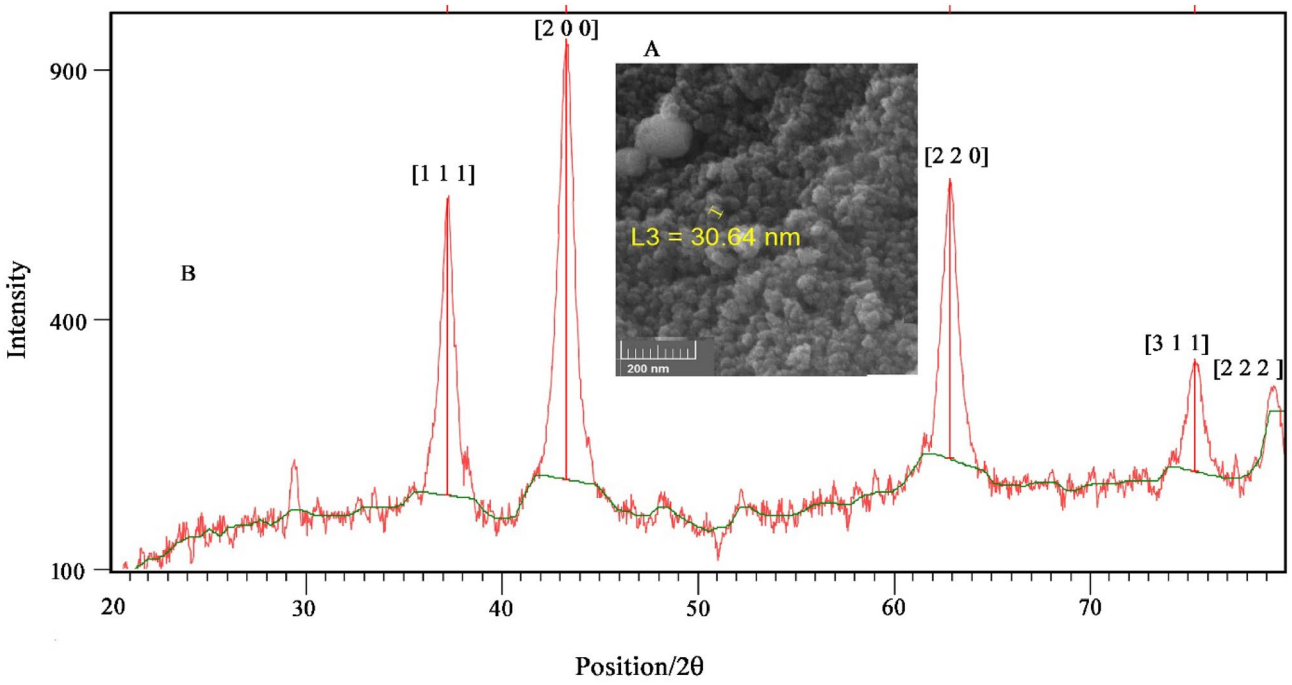

Figure 2. **(A)** FESEM image and **(B)** XRD pattern of NiO dope Pt nanostructure hybrid.

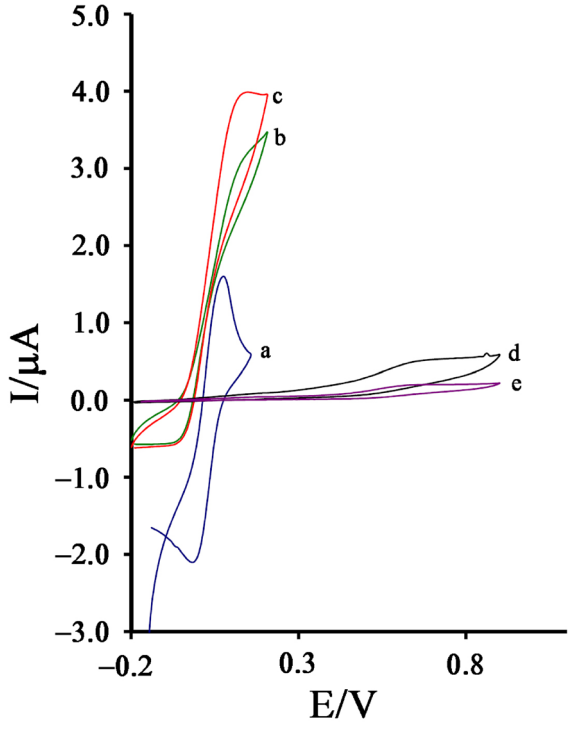

Figure 3. **(a)** Cyclic voltammogram of NiO–Pt–H/B,1,10,P,1,10,PDNiPF6/CPE in the PBS (pH 7.0). **(b)** Cyclic voltammogram of B,1,10,P,1,10,PDNiPF6/CPE in the presence of 500 μM cysteamine. **(c)** Cyclic voltammogram of NiO–Pt–H/B,1,10,P,1,10,PDNiPF6/CPE in the presence of 500 μM cysteamine. **(d)** Cyclic voltammogram of NiO–Pt–H/CPE in the presence of 500 μM cysteamine and **(e)** cyclic voltammogram of CPE in the presence of 500 μM cysteamine (condition; pH 7.0, scan rate 10 mV/s).

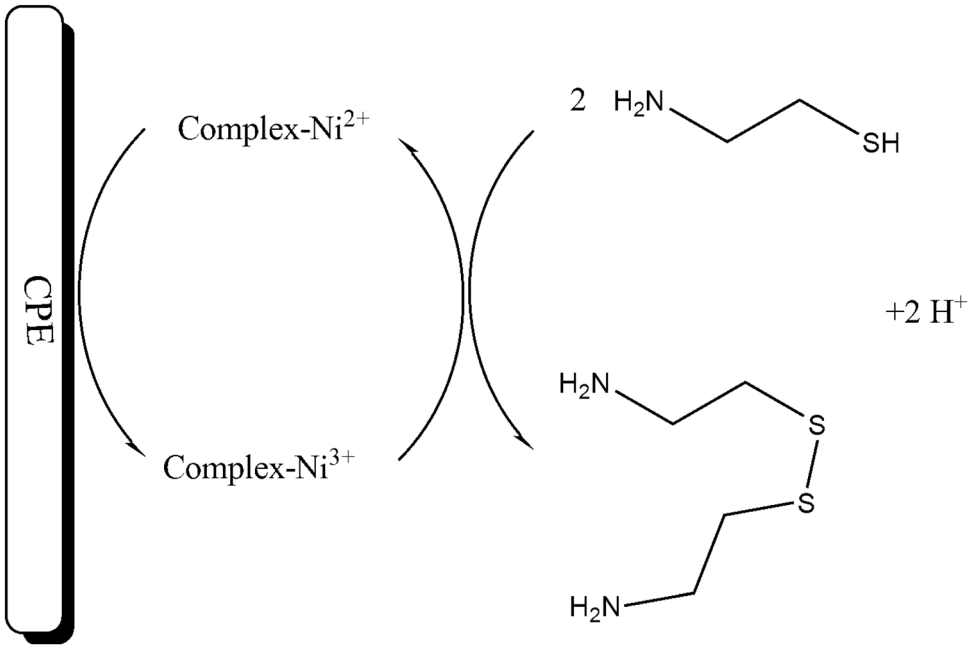

Scheme 1. Electrocatalytic mechanism for determination of cysteamine on the surface of NiO–Pt–H/B,1,10,P,1,10,PDNiPF6/CPE.

the electrode surface. In the same solution and on the surface of CPE (Fig. 3, curve e), a low oxidation signal at potential ~ 620 mV relative to electrooxidation of cysteamine can be observed.

After modification of CPE with NiO–Pt–H and on the surface of NiO–Pt–H/CPE, the oxidation signal of cysteamine was increased, but a small decrease was observed in oxidation potential of cysteamine (Fig. 3, curve d). Comparison of curve "c" with curve "e" properly indicates that measurement of cysteamine at a potential of about 500 mV is less positive than its actual value at unmodified electrode with greater sensitivity which can be possible on the surface of NiO–Pt–H/B,1,10,P,1,10,PDNiPF6/CPE.

The cyclic voltammograms 200 µM cysteamine on the surface of NiO–Pt–H/B,1,10,P,1,10,PDNiPF6/CPE in the scan range of 3.0–20.0 mV/s was recorded and the results are presented in Fig. 4 inset. According to equation $I_{pa} = 0.607\ \nu^{1/2} - 0.6265$ ($R^2 = 0.9969$), a linear relation was observed between the oxidation signal of cysteamine and $\nu^{1/2}$ on the surface of NiO–Pt–H/B,1,10,P,1,10,PDNiPF6/CPE (Fig. 4). This linear relation confirms a diffusion process[68–70] for electro-oxidation of cysteamine on the surface of NiO–Pt–H/B,1,10,P,1,10,PDNiPF6/CPE.

The value electron transfer coefficient (α) as a kinetic parameter, containing useful information about the rate-determining step, was calculated by the Tafel plot (Fig. 5). The slope of the Tafel plot relative electrooxidation 600 µM cysteamine on the surface of NiO–Pt–H/B,1,10,P,1,10,PDNiPF6/CPE was equal to $2.3RT/n(1 - \alpha)F$, which came up to 0.122 V decade^{-1} for scan rates of 10 mV s^{-1}. The value of α for cysteamine was determined as ~ 0.52.

The Electrochemical impedance spectroscopy (EIS) technique was used to confirm the electro-catalytic process between B,1,10,P,1,10,PDNiPF6 and cysteamine on the surface of NiO–Pt–H/B,1,10,P,1,10,PDNiPF6/CPE (Fig. 6). The Nyquist diagrams of NiO–Pt–H/B,1,10,P,1,10,PDNiPF6/CPE in the absence (curve a) and presence of 1.0 mM cysteamine (curve b) and 1.0 mM serotonin (curve c) are presented in Fig. 6, respectively. As can be seen, the diameter of the semicircle (relative to charge transfer resistance) relative to NiO–Pt–H/B,1,10,P,1,10,PDNiPF6/CPE in the absence and presence of 1.0 mM serotonin are very similar, confirming that no electrocatalytic reaction took place between serotonin and mediator on the surface of NiO–Pt–H/B,1,10,P,1,10,PDNiPF6/CPE. After the addition of 1.0 mM cysteamine (curve b), the diameter of the semicircle was decreased on the surface of NiO–Pt–H/B,1,10,P,1,10,PDNiPF6/CPE. This point is relative to the electrocatalytic reaction between mediator and cysteamine, increasing in oxidation signal of the mediator and decreasing in charge transfer resistance of electrode surface.

Chronoamperometric investigation. The value of diffusion coefficient (D) and catalytic rate constant, kh were determined using chronoamperogram recording of NiO–Pt–H/B,1,10,P,1,10,PDNiPF6/CPE in the absence of (Fig. 7A, curve a) and in the presence of 50 µM (Fig. 7A, curve b) and 100 µM (Fig. 7A, curve c) cysteamine, using applied potential – 0.1 and 0.2 mV. The value of D was determined by recording Cottrell plots relative to chronoamperogram which was recorded in the presence of cysteamine (Fig. 7B). The slopes and Cottrell equation (Eq. 1):

$$I = \frac{nFAD^{1/2}C}{\pi^{1/2}} t^{-1/2} \quad (1)$$

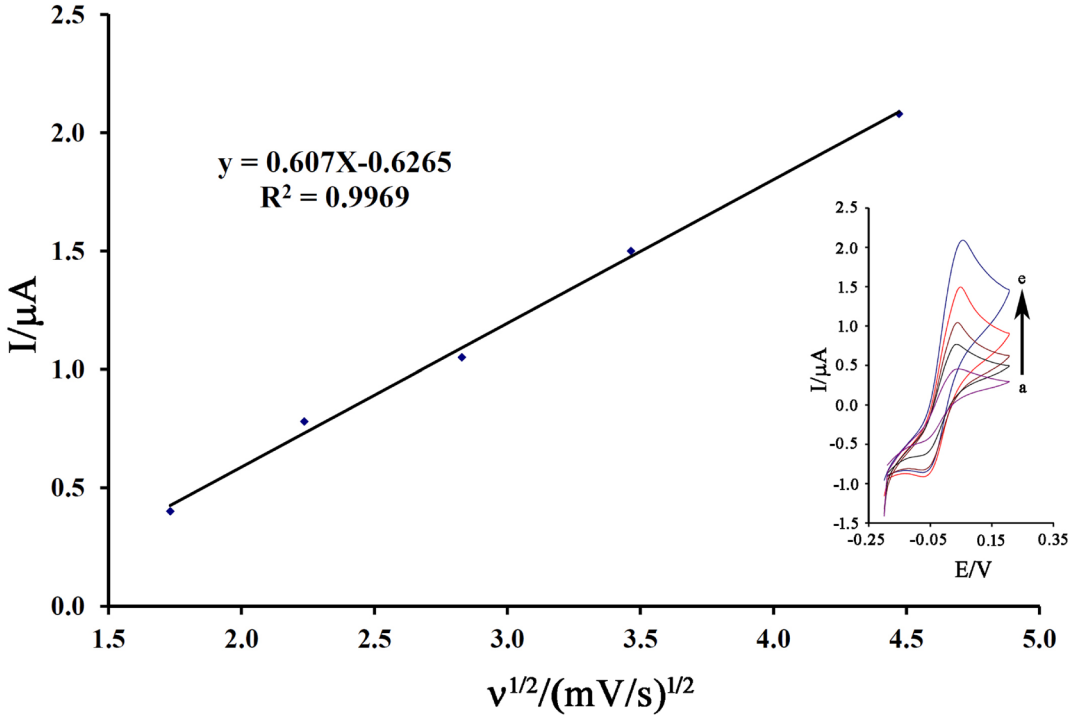

Figure 4. The plot of I vs. $\nu^{1/2}$ for electro-oxidation 200 μM cysteamine on the surface of NiO–Pt–H/B,1,10,P,1,10,PDNiPF6/CPE in the scans **(a)** 3; **(b)** 5; **(c)** 8; **(d)** 12 and **(e)** 20 mV/s.

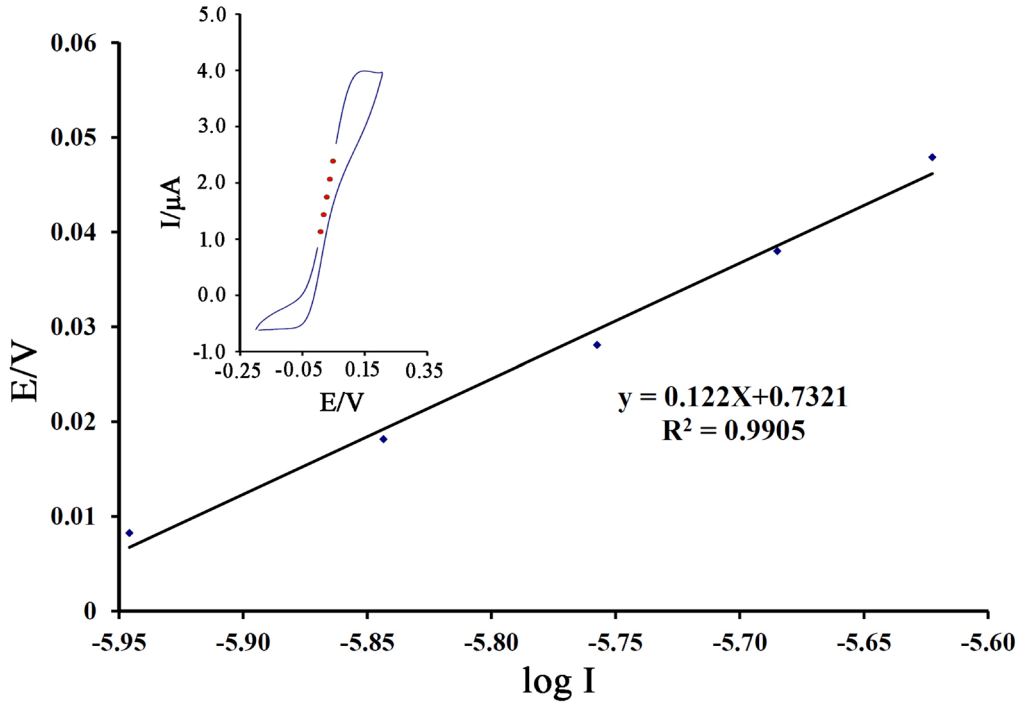

Figure 5. Tafel plot for NiO–Pt–H/B,1,10,P,1,10,PDNiPF6/CPE in (pH 7.0) with a scan rate of 10 mV/s in the presence of 500 μM cysteamine.

The mean value of D for cysteamine was determined as ~ 2.45×10^{-5} cm^2/s.

The catalytic rate constant between B,1,10,P,1,10,PDNiPF6 and cysteamine can be determined according to the method of Galus equation (Eq. 2):

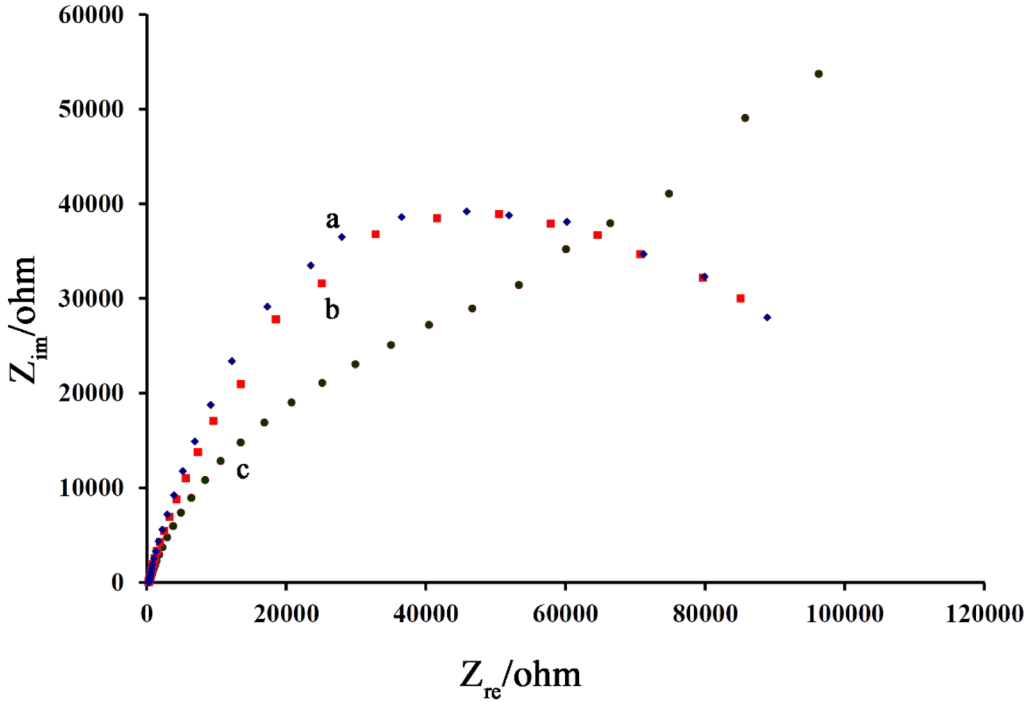

Figure 6. Nyquist diagrams of NiO–Pt–H/B,1,10,P,1,10,PDNiPF6/CPE in the absence **(a)** and in the presence **(b)** of 1.0 mM serotonin and **(c)** with 1.0 mM cysteamine.

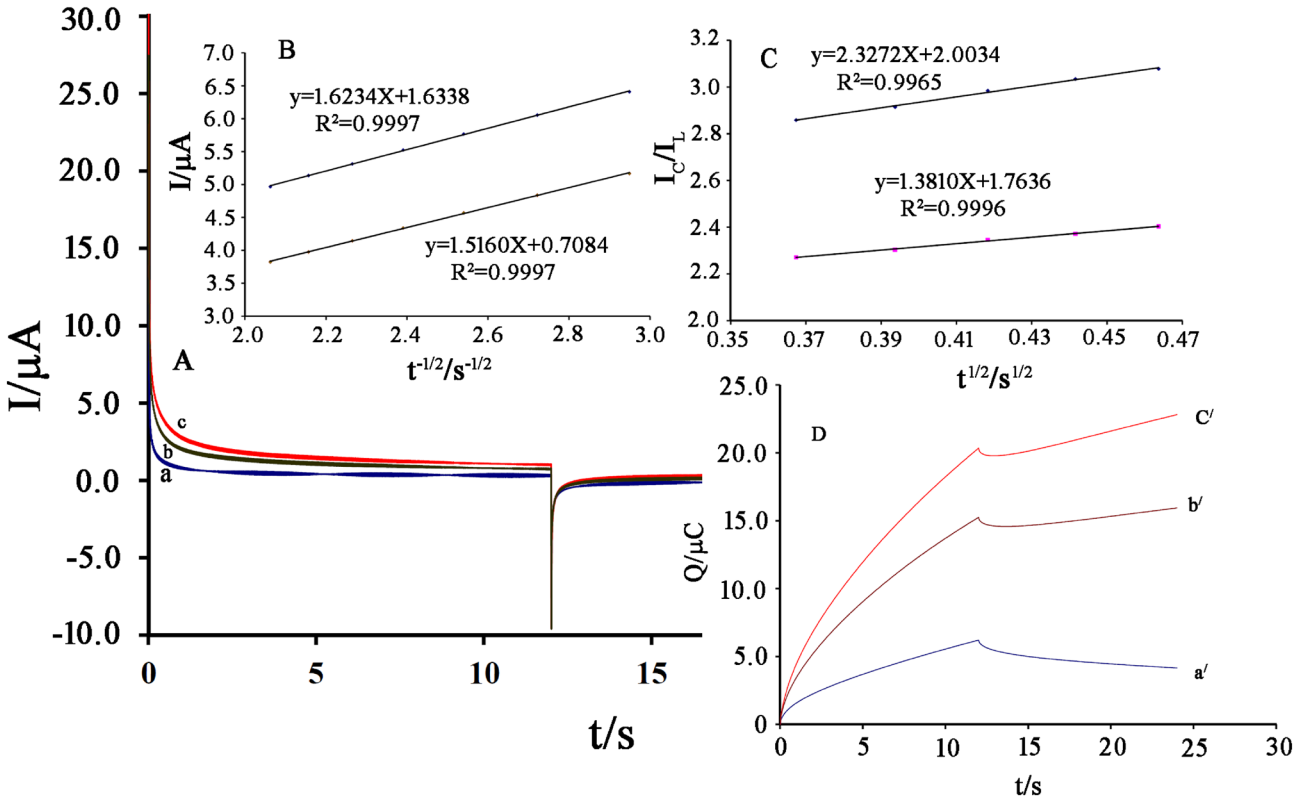

Figure 7. **(A)** Chronoamperograms obtained at NiO–Pt–H/B,1,10,P,1,10,PDNiPF6/CPE **(a)** in the absence, **(b)** in the presence of 50.0 μM and **(c)** in the presence of 100.0 cysteamine at pH 7.0. **(B)** Cottrell's plot for cysteamine oxidation data on the surface of NiO–Pt–H/B,1,10,P,1,10,PDNiPF6/CPE. **(C)** Dependence of I_c/I_L on the $t^{1/2}$ derived from the chronoamperogram data. **(D)** The charge–time curves derived from the chronoamperogram data.

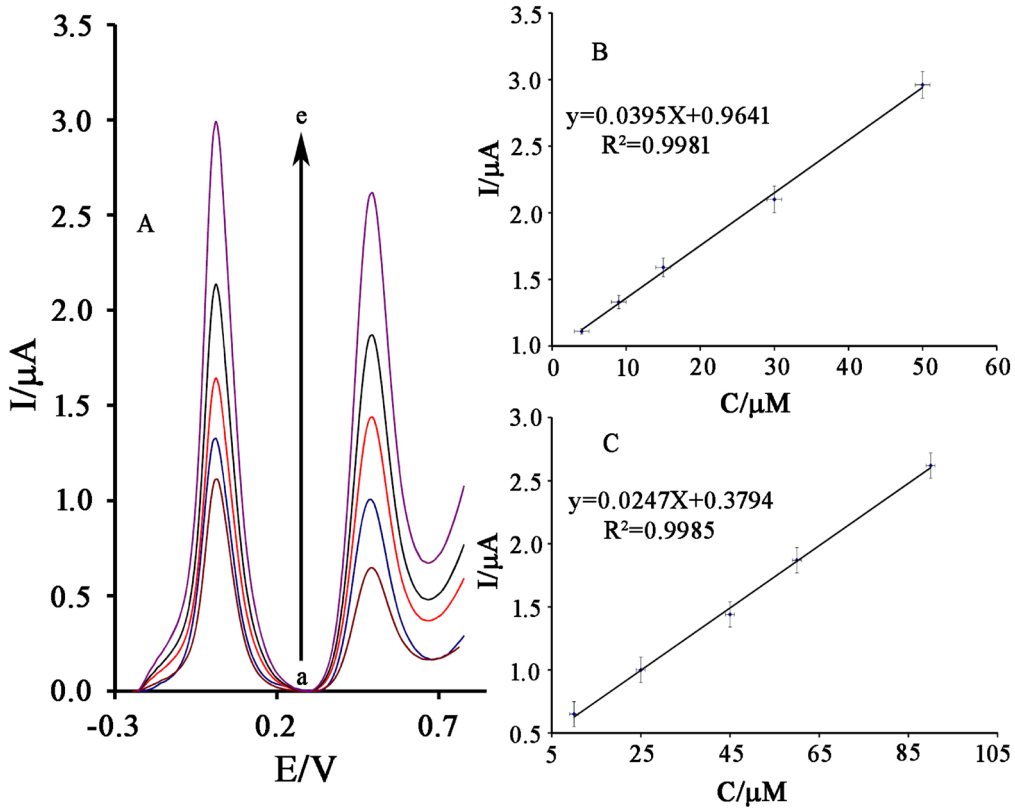

Figure 8. **(A)** SWVs of NiO–Pt–H/B,1,10,P,1,10,PDNiPF6/CPE containing different concentrations of cysteamine–serotonin in μM (from inner to outer): 4.0 + 10.0; 9.0 + 25.0; 15.0 + 45.0; 30.0 + 60.0 and 50.0 + 90.0, respectively. Insets: Plots of I_p vs. **(B)** cysteamine and **(C)** serotonin concentrations.

$$\frac{I_C}{I_L} = \gamma^{1/2}\pi^{1/2} = \pi^{1/2}(k_h Ct)^{1/2} \quad (2)$$

Based on the slope reported from the I_C/I_L (I_C is catalytic current in the presence of cysteamine and I_L oxidation current in the absence of cysteamine) vs. $t^{1/2}$ and Eq. (2), the value of k_h can be determined 1.4732×10^4 mol^{-1} L s^{-1} (Fig. 7C).

Chronocoulometry technique (double potential step) was also used for the examination of electrode processes at NiO–Pt–H/B,1,10,P,1,10,PDNiPF6/CPE (Fig. 7D). Forward and backward charge on the NiO–Pt–H/B,1,10,P,1,10,PDNiPF6/CPE in a blank buffer solution showed very symmetrical chronocoulograms. This recorded signal confirms an equal charge consumed for redox reaction of the Ni^{2+}/Ni^{3+} system in NiO–Pt–H/B,1,10,P,1,10,PDNiPF6/CPE. However, after the addition of cysteamine, the value of oxidation charge value in chronocoulometric investigation was increased and the backward charge value in chronocoulometric investigation was decreased. These changes properly illustrate the electrocatalytic process.

Simultaneous determination of cysteamine and serotonin. The square wave voltammograms (SWV) of cysteamine and serotonin were recorded separately on the surface of NiO–Pt–H/B,1,10,P,1,10,PDNiPF6/CPE. The results showed a linear relation between oxidation current of cysteamine and its concentration in the range of 0.003–200 μM with equation $I_{pa} = 0.0385\ C_{cysteamine} + 0.9602$ ($R^2 = 0.9978$) and a linear range between 0.5 and 260 μM with equation $I_{pa} = 0.0238\ C_{Serotonin} + 0.4139$ ($R^2 = 0.9969$) for the determination of serotonin on the surface of NiO–Pt–H/B,1,10,P,1,10,PDNiPF6/CPE. The detection limit (LOD) was 0.5 nM cysteamine and 0.1 μM serotonin, according to the definition of LOD = 3sb/m.

On the other hand, the square wave voltammograms of NiO–Pt–H/B,1,10,P,1,10,PDNiPF6/CPE in the solution containing different concentrations of cysteamine and serotonin was recorded and the obtained signals were presented in Fig. 8A. As can be seen, we detected two separated oxidation signals relative to cysteamine and serotonin at potentials of 10 mV and 495 mV with ΔE = 485 mV that is very interesting for the simultaneous determination of the two compounds using NiO–Pt–H/B,1,10,P,1,10,PDNiPF6/CPE. On the other hand, the oxidation potential of cysteamine and serotonin is very close to each other on the surface of the carbon paste electrode (Fig. 9). The linear relation between oxidation signal of cysteamine and serotonin and their concentration in this investigation are presented in Fig. 8B, C. Slopes of 0.0395 μA/μM and 0.0247 μA/μM for cysteamine and serotonin were obtained, respectively. These sensitivities are very similar to the sensitivity recorded for

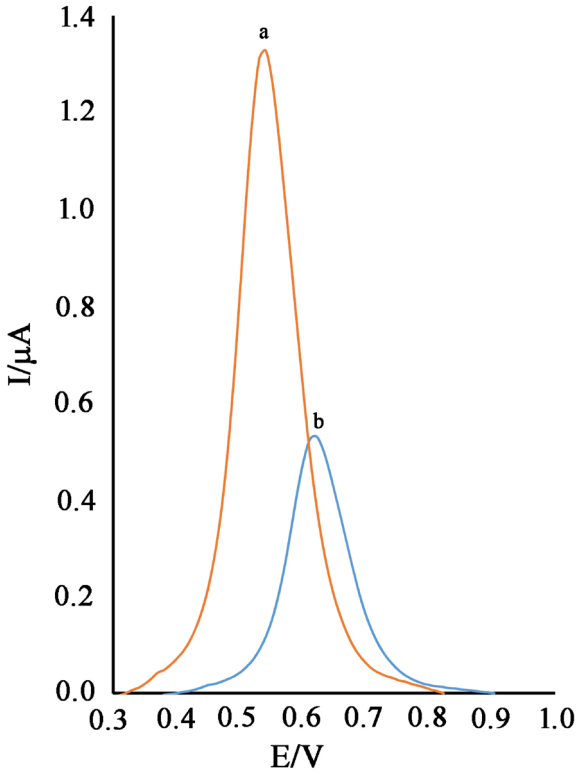

Figure 9. SWVs of carbon paste electrode in the solution containing **(a)** 500 μM serotonin and **(b)** 500 μM cysteamine.

cysteamine and serotonin in linear dynamic range investigation, confirming that the determination of cysteamine and serotonin can be done successfully without any interference in the mixed samples.

Stability and reproducibility. The reproducibility and stability of NiO–Pt–H/B,1,10,P,1,10,PDNiPF6/CPE were investigated by recording SWV of 100.0 μM cysteamine at pH 7.0. We detected a relative standard deviation of (RSD%) 2.1% for five successive recorded signals that confirmed good repeatability for NiO–Pt–H/B,1,10,P,1,10,PDNiPF6/CPE as an electroanalytical sensor. Moreover, the stability of the NiO–Pt–H/B,1,10,P,1,10,PDNiPF6/CPE was examined by the storage of the sensor in the lab. Then, NiO–Pt–H/B,1,10,P,1,10,PDNiPF6/CPE was used for the determination of 100.0 μM cysteamine using SWV. The recorded signal showed 93.2% of its initial response relative to 100.0 μM cysteamine after 60 days, using NiO–Pt–H/B,1,10,P,1,10,PDNiPF6/CPE, indicating good stability for the suggested sensor. To study the reproducibility of NiO–Pt–H/B,1,10,P,1,10,PDNiPF6/CPE in determination of 500 μM cysteamine, five modified electrodes were prepared in the same condition and the oxidation signal of cysteamine was recorded on the surface of NiO–Pt–H/B,1,10,P,1,10,PDNiPF6/CPE with a scan rate of 10 mV/s. A relative standard deviation of (RSD%) 3.33% was detected for the determination of cysteamine on the surface of these electrodes, confirming good reproducibility for the fabrication of NiO–Pt–H/B,1,10,P,1,10,PDNiPF6/CPE (Fig. 10).

Real sample and interference study. The selectivity of NiO–Pt–H/B,1,10,P,1,10,PDNiPF6/CPE as an electroanalytical sensor was checked in the solution containing 20.0 μM cysteamine with an acceptable error of 5% in oxidation current. The results are presented in Table 1 and the data obtained exhibit interesting selection of NiO–Pt–H/B,1,10,P,1,10,PDNiPF6/CPE as an electroanalytical sensor for the determination of cysteamine.

In the final step, we check the ability of NiO–Pt–H/B,1,10,P,1,10,PDNiPF6/CPE as a powerful electroanalytical sensor for determination of cysteamine and serotonin in capsule and pharmaceutical serum samples. The recovery data between 98.5–103.06% for analysis of cysteamine and 98.1–101.68% for analysis of serotonin were observed on the surface of NiO–Pt–H/B,1,10,P,1,10,PDNiPF6/CPE (Table 2), confirming the powerful ability of NiO–Pt–H/B,1,10,P,1,10,PDNiPF6/CPE as a novel and powerful analytical sensor.

Conclusion

In this study, a novel and highly sensitive electroanalytical sensor was fabricated for the determination of cysteamine by modification of CPE with NiO–Pt–H and B,1,10,P,1,10,PDNiPF6 as two mediators. The NiO–Pt–H was synthesized by an one-pot procedure resulting in a spherical shape with diameter of 30.64 nm. The NiO–Pt–H/B,1,10,P,1,10,PDNiPF6/CPE was used as the first electrochemical sensor for the simultaneous analysis of cysteamine and serotonin with detection limits of 0.5 nM and 0.1 μM, respectively. In addition,

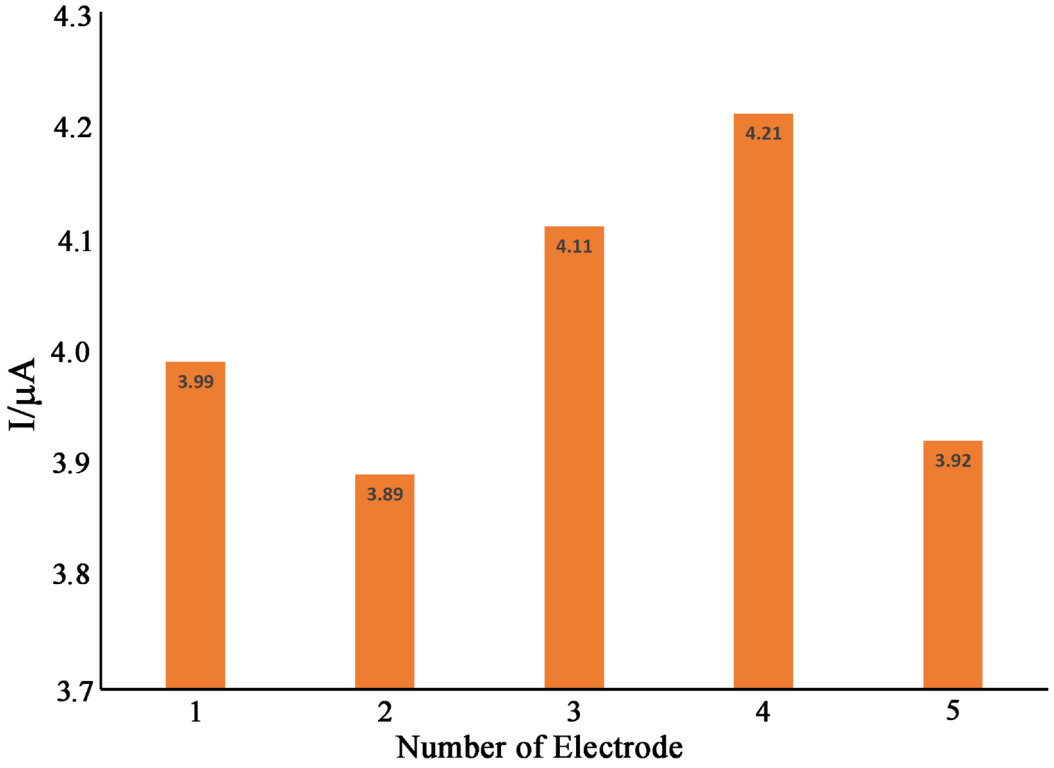

Figure 10. Recorded current for electrooxidation of 500 μM cysteamine on the surface of five different NiO–Pt–H/B,1,10,P,1,10,PDNiPF6/CPEs prepared in the same condition.

Species	Tolerant limits ($W_{interference}/W_{cysteamine}$)
Cl^-, K^+, Li^+, F^-, Mg^{2+}	950
Fructose and glucose, ascorbic acid (after addition of 1.0 mM ascorbate oxidase)	750
Methionine, Dopamine, Valine, Uric acid, vitamin B_2	300

Table 1. The interference study results in the presence of 20.0 μM cysteamine.

Samples	Cysteamine standard solution added (μM)	Serotonin standard solution added (μM)	Founded of cysteamine (μM)	Founded of serotonin (μM)	Recovery value % for cysteamine	Recovery value % for serotonin
Cysteamine capsule	–	–	–	4.95 ± 0.45	–	–
	5.00	–	9.83 ± 0.67	–	98.79	–
Pharmaceutical serum	–	–	< LOD	< LOD	–	–
	10.00	10.00	9.85 ± 0.39	9.81 ± 0.52	98.5	98.1
	15.00	45.00	15.46 ± 0.59	45.76 ± 0.93	103.06	101.68

Table 2. Determination of cysteamine and serotonin in real samples (n = 5).

NiO–Pt–H and B,1,10,P,1,10,PDNiPF6 showed a powerful ability for the determination of cysteamine and serotonin in the drug and pharmaceutical serum samples with recovery data of 98.1–103.06%.

Received: 7 March 2020; Accepted: 1 July 2020
Published online: 16 July 2020

References

1. Karimi-Maleh, H., Biparva, P. & Hatami, M. A novel modified carbon paste electrode based on NiO/CNTs nanocomposite and (9, 10-dihydro-9, 10-ethanoanthracene-11, 12-dicarboximido)-4-ethylbenzene-1, 2-diol as a mediator for simultaneous determination of cysteamine, nicotinamide adenine dinucleotide and folic acid. *Biosens. Bioelectron.* **48**, 270–275 (2013).
2. Healy, J. A trial of cystamine in radiation sickness. *Br. J. Radiol.* **33**(392), 512–514 (1960).

3. Vecsei, L., Kovacs, G., Faludi, M., Bollok, I. & Telegdy, G. Dose-related effects of cysteamine treatment on hypothalamic and striatal dopamine, noradrenaline and serotonin neurotransmission. *Acta Physiol. Hung.* **66**(2), 213–217 (1985).
4. Szabo, S. *et al.* Biochemical changes in tissue catecholamines and serotonin in duodenal ulceration caused by cysteamine or propionitrile in the rat. *J. Pharmacol. Exp. Ther.* **240**(3), 871–878 (1987).
5. Sharma, S., Singh, N., Tomar, V. & Chandra, R. A review on electrochemical detection of serotonin based on surface modified electrodes. *Biosens. Bioelectron.* **107**, 76–93 (2018).
6. Koch, D. D. & Kissinger, P. T. Determination of serotonin in serum and plasma by liquid chromatography with precolumn sample enrichment and electrochemical detection. *Anal. Chem.* **52**(1), 27–29 (1980).
7. Satyanarayana, M., Koteshwara Reddy, K. & Vengatajalabathy Gobi, K. Nanobiocomposite based electrochemical sensor for sensitive determination of serotonin in presence of dopamine, ascorbic acid and uric acid in vitro. *Electroanalysis* **26**(11), 2365–2372 (2014).
8. Kelly, M. J., Perrett, D. & Rudge, S. R. The determination of cysteamine in physiological fluids by HPLC with electrochemical detection. *Biomed. Chromatogr.* **2**(5), 216–220 (1987).
9. Kubalczyk, P. & Bald, E. Method for determination of total cysteamine in human plasma by high performance capillary electrophoresis with acetonitrile stacking. *Electrophoresis* **29**(17), 3636–3640 (2008).
10. Tumur, M., Kanberoglu, G. S. & Coldur, F. A novel potentiometric PVC-membrane cysteamine-selective electrode based on cysteamine-phosphomolybdate ion-pair. *Curr. Pharm. Anal.* **16**(2), 168–175 (2020).
11. Kataoka, H., Imamura, Y., Tanaka, H. & Makita, M. Determination of cysteamine and cystamine by gas chromatography with flame photometric detection. *J. Pharm. Biomed. Anal.* **11**(10), 963–969 (1993).
12. Apyari, V. V., Dmitrienko, S. G., Arkhipova, V. V., Atnagulov, A. G. & Zolotov, Y. A. Determination of cysteamine using label-free gold nanoparticles. *Anal. Methods* **4**(10), 3193–3199 (2012).
13. Rezaei, B., Khosropour, H. & Ensafi, A. A. Sensitive voltammetric determination of cysteamine using promazine hydrochloride as a mediator and modified multi-wall carbon nanotubes carbon paste electrodes. *Ionics* **20**(9), 1335–1342 (2014).
14. Mollarasouli, F., Kurbanoglu, S. & Ozkan, S. A. The role of electrochemical immunosensors in clinical analysis. *Biosensors* **9**(3), 86 (2019).
15. S. Kaya, B. Demirkan, N. Bakirhan, E. Kuyuldar, S. Kurbanoglu, S. Ozkan, F. Sen, Highly sensitive carbon-based nanohybrid sensor platform for determination of 5-hydroxytryptamine receptor agonist (Eletriptan). J. Pharmaceut. Biomed. Anal. (2019).
16. H. Karimi-Maleh, F. Karimi, M. Alizadeh, A.L. Sanati, Electrochemical sensors, a bright future in the fabrication of portable kits in analytical systems. Chem. Rec. **20**. https://doi.org/10.1002/tcr.201900092 (2020).
17. Soltani, H., Beitollahi, H., Hatefi-Mehrjardi, A.-H., Tajik, S. & Torkzadeh-Mahani, M. Voltammetric determination of glutathione using a modified single walled carbon nanotubes paste electrode. *Anal. Bioanal. Electrochem* **6**(1), 67–79 (2014).
18. Beitollahi, H. *et al.* Application of graphite screen printed electrode modified with dysprosium tungstate nanoparticles in voltammetric determination of epinephrine in the presence of acetylcholine. *J. Rare Earths* **36**(7), 750–757 (2018).
19. Motaghi, M. M., Beitollahi, H., Tajik, S. & Hosseinzadeh, R. Nanostructure electrochemical sensor for voltammetric determination of vitamin C in the presence of vitamin B6: Application to real sample analysis. *Int. J. Electrochem. Sci* **11**, 7849–7860 (2016).
20. Baghbamidi, S. E., Beitollahi, H., Tajik, S. & Hosseinzadeh, R. Voltammetric sensor based on 1-benzyl-4-ferrocenyl-1H-[1, 2, 3]-triazole/carbon nanotube modified glassy carbon electrode; detection of hydrochlorothiazide in the presence of propranolol. *Int. J. Electrochem. Sci.* **11**(12), 10874–10883 (2016).
21. Bakirhan, N. K., Ozcelikay, G. & Ozkan, S. A. Recent progress on the sensitive detection of cardiovascular disease markers by electrochemical-based biosensors. *J. Pharm. Biomed. Anal.* **159**, 406–424 (2018).
22. Keyvanfard, M., Ahmadi, M., Karimi, F. & Alizad, K. Voltammetric determination of cysteamine at multiwalled carbon nanotubes paste electrode in the presence of isoproterenol as a mediator. *Chin. Chem. Lett.* **25**(9), 1244–1246 (2014).
23. Mazloum-Ardakani, M. *et al.* Application of 2-(3, 4-dihydroxyphenyl)-1, 3-dithialone self-assembled monolayer on gold electrode as a nanosensor for electrocatalytic determination of dopamine and uric acid. *Analyst* **136**(9), 1965–1970 (2011).
24. Karimi-Maleh, H. *et al.* A high sensitive biosensor based on FePt/CNTs nanocomposite/N-(4-hydroxyphenyl)-3, 5-dinitrobenzamide modified carbon paste electrode for simultaneous determination of glutathione and piroxicam. *Biosens. Bioelectron.* **60**, 1–7 (2014).
25. Ensafi, A. A., Karimi-Maleh, H. & Mallakpour, S. Simultaneous determination of ascorbic acid, acetaminophen, and tryptophan by square wave voltammetry using N-(3, 4-dihydroxyphenethyl)-3, 5-dinitrobenzamide-modified carbon nanotubes paste electrode. *Electroanalysis* **24**(3), 666–675 (2012).
26. Ensafi, A. A. & Maleh, H. K. A multiwall carbon nanotubes paste electrode as a sensor and ferrocenemonocarboxylic acid as a mediator for electrocatalytic determination of isoproterenol. *Int. J. Electrochem. Sci* **5**, 1484–1495 (2010).
27. Raoof, J. B., Ojani, R., Karimi-Maleh, H., Hajmohamadi, M. R. & Biparva, P. Multi-wall carbon nanotubes as a sensor and ferrocene dicarboxylic acid as a mediator for voltammetric determination of glutathione in hemolysed erythrocyte. *Anal. Methods* **3**(11), 2637–2643 (2011).
28. Ensafi, A. A. & Karimi-Maleh, H. A voltammetric sensor based on modified multiwall carbon nanotubes for cysteamine determination in the presence of tryptophan using p-aminophenol as a mediator. *Electroanalysis* **22**(21), 2558–2568 (2010).
29. Karimi-Maleh, H., Ensafi, A. A. & Ensafi, H. R. Ferrocenedicarboxylic acid modified carbon paste electrode: A sensor for electrocatalytic determination of hydrochlorothiazide. *J. Braz. Chem. Soc.* **20**(5), 880–887 (2009).
30. Karimi-Maleh, H. *et al.* Palladium-Nickel nanoparticles decorated on functionalized-MWCNT for high precision non-enzymatic glucose sensing. *Mater. Chem. Phys.* **250**, 123042 (2020).
31. Ensafi, A. A., Karimi-Maleh, H. & Mallakpour, S. N-(3, 4-dihydroxyphenethyl)-3, 5-dinitrobenzamide-modified multiwall carbon nanotubes paste electrode as a novel sensor for simultaneous determination of penicillamine, uric acid, and tryptophan. *Electroanalysis* **23**(6), 1478–1487 (2011).
32. Ensafi, A., Karimi-Maleh, H. & Mallakpour, S. A new strategy for the selective determination of glutathione in the presence of nicotinamide adenine dinucleotide (NADH) using a novel modified carbon nanotube paste electrode. *Colloids Surf. B* **104**, 186–193 (2013).
33. Ensafi, A. A., Dadkhah-Tehrani, S. & Karimi-Maleh, H. A voltammetric sensor for the simultaneous determination of L-cysteine and tryptophan using a p-aminophenol-multiwall carbon nanotube paste electrode. *Anal. Sci.* **27**(4), 409–409 (2011).
34. Raoof, J.-B., Ojani, R. & Baghayeri, M. Simultaneous electrochemical determination of glutathione and tryptophan on a nano-TiO_2/ferrocene carboxylic acid modified carbon paste electrode. *Sens. Actuators B Chem.* **143**(1), 261–269 (2009).
35. Karimi-Maleh, H. *et al.* Electrocatalytic and simultaneous determination of ascorbic acid, nicotinamide adenine dinucleotide and folic acid at ruthenium (II) complex-ZnO/CNTs nanocomposite modified carbon paste electrode. *Electroanalysis* **26**(5), 962–970 (2014).
36. Karimi-Maleh, H., Ahanjan, K., Taghavi, M. & Ghaemy, M. A novel voltammetric sensor employing zinc oxide nanoparticles and a new ferrocene-derivative modified carbon paste electrode for determination of captopril in drug samples. *Anal. Methods* **8**(8), 1780–1788 (2016).
37. Baghayeri, M., Rouhi, M., Lakouraj, M. M. & Amiri-Aref, M. Bioelectrocatalysis of hydrogen peroxide based on immobilized hemoglobin onto glassy carbon electrode modified with magnetic poly (indole-co-thiophene) nanocomposite. *J. Electroanal. Chem.* **784**, 69–76 (2017).

38. Shabani-Nooshabadi, M. & Tahernejad-Javazmi, F. Electrocatalytic determination of hydroxylamine in the presence of thiosulfate in water and wastewater samples using a nanostructure modified carbon paste electrode. *Electroanalysis* **27**(7), 1733–1741 (2015).
39. Shabani-Nooshabadi, M. & Tahernejad-Javazmi, F. Rapid and fast strategy for the determination of glutathione in the presence of vitamin B 6 in biological and pharmaceutical samples using a nanostructure based electrochemical sensor. *RSC Adv.* **5**(69), 56255–56261 (2015).
40. Tahernejad-Javazmi, F. & Shabani-Nooshabadi, M. Voltammetric determination of thiosulfate in presence of p-nitrophenol using an electrochemical nanostructure sensor modified with a new mediator. *J. Electrochem. Soc.* **164**(13), H975–H980 (2017).
41. Baghayeri, M., Namadchian, M., Karimi-Maleh, H. & Beitollahi, H. Determination of nifedipine using nanostructured electrochemical sensor based on simple synthesis of Ag nanoparticles at the surface of glassy carbon electrode: Application to the analysis of some real samples. *J. Electroanal. Chem.* **697**, 53–59 (2013).
42. Shabani-Nooshabadi, M., Roostaee, M. & Tahernejad-Javazmi, F. Graphene oxide/NiO nanoparticle composite-ionic liquid modified carbon paste electrode for selective sensing of 4-chlorophenol in the presence of nitrite. *J. Mol. Liq.* **219**, 142–148 (2016).
43. Fouladgar, M. *et al.* Voltammetric determination of amoxicillin at the electrochemical sensor ferrocenedicarboxylic acid multi wall carbon nanotubes paste electrode. *Int. J. Electrochem. Sci.* **6**, 1355–1366 (2011).
44. Fouladgar, M. Electrocatalytic measurement of trace amount of captopril using multiwall carbon nanotubes as a sensor and ferrocene as a mediator. *Int. J. Electrochem. Sci* **6**, 705–716 (2011).
45. Golikand, A. N., Raoof, J., Baghayeri, M., Asgari, M. & Irannejad, L. Nickel electrode modified by *N*, *N*-bis (salicylidene) phenylenediamine (Salophen) as a catalyst for methanol oxidation in alkaline medium. *Russ. J. Electrochem.* **45**(2), 192–198 (2009).
46. Maleki, B. & Baghayeri, M. Synthesis of symmetrical *N, N′*-alkylidene bis-amides catalyzed by silica coated magnetic $NiFe_2O_4$ nanoparticle supported polyphosphoric acid ($NiFe_2O_4$ @ SiO_2-PPA) and its application toward silver nanoparticle synthesis for electrochemical detection of glucose. *RSC Adv.* **5**(97), 79746–79758 (2015).
47. Li, Y. *et al.* Carboxyl-functionalized mesoporous molecular sieve/colloidal gold modified nano-carbon ionic liquid paste electrode for electrochemical determination of serotonin. *Mater. Res. Bull.* **109**, 240–245 (2019).
48. Fouladgar, M. CuO-CNT nanocomposite/ionic liquid modified sensor as new breast anticancer approach for determination of doxorubicin and 5-fluorouracil drugs. *J. Electrochem. Soc.* **165**(13), B559–B564 (2018).
49. Lu, Y. *et al.* Aptamer-based electrochemical sensors with aptamer—Complementary DNA oligonucleotides as probe. *Anal. Chem.* **80**(6), 1883–1890 (2008).
50. Kwon, H., Chan, K. M. & Kool, E. T. DNA as an environmental sensor: Detection and identification of pesticide contaminants in water with fluorescent nucleobases. *Org. Biomol. Chem.* **15**(8), 1801–1809 (2017).
51. Feng, K.-J. *et al.* A nano-porous CeO_2/chitosan composite film as the immobilization matrix for colorectal cancer DNA sequence-selective electrochemical biosensor. *Talanta* **70**(3), 561–565 (2006).
52. Jahandari, S., Taher, M. A., Karimi-Maleh, H. & Mansouri, G. Simultaneous voltammetric determination of glutathione, doxorubicin and tyrosine based on the electrocatalytic effect of a nickel (II) complex and of Pt:Co nanoparticles as a conductive mediator. *Microchim. Acta* **186**(8), 493 (2019).
53. Baghayeri, M. Pt nanoparticles/reduced graphene oxide nanosheets as a sensing platform: Application to determination of droxidopa in presence of phenobarbital. *Sens. Actuators B Chem.* **240**, 255–263 (2017).
54. Veisi, H., Eshbala, F. H., Hemmati, S. & Baghayeri, M. Selective hydrogen peroxide oxidation of sulfides to sulfones with carboxylated multi-walled carbon nano tubes (MWCNTs-COOH) as heterogeneous and recyclable nanocatalysts under organic solvent-free conditions. *RSC Adv.* **5**(14), 10152–10158 (2015).
55. Beitollahi, H., Tajik, S., Mohammadi, S. Z. & Baghayeri, M. Voltammetric determination of hydroxylamine in water samples using a 1-benzyl-4-ferrocenyl-1H-[1, 2, 3]-triazole/carbon nanotube-modified glassy carbon electrode. *Ionics* **20**(4), 571–579 (2014).
56. Baghayeri, M. *et al.* Multi-walled carbon nanotubes decorated with palladium nanoparticles as a novel platform for electrocatalytic sensing applications. *RSC Adv.* **4**(91), 49595–49604 (2014).
57. Khalilzadeh, M. A., Karimi-Maleh, H., Amiri, A. & Gholami, F. Determination of captopril in patient human urine using ferrocenemonocarboxylic acid modified carbon nanotubes paste electrode. *Chin. Chem. Lett.* **21**(12), 1467–1470 (2010).
58. Fu, L. *et al.* Lycoris species identification and infrageneric relationship investigation via graphene enhanced electrochemical fingerprinting of pollen. *Sens. Actuators B Chem.* **298**, 126836 (2019).
59. Yuan, B. *et al.* Pd nanoparticles supported on 1, 10-phenanthroline-5, 6-dione modified graphene oxide as superior bifunctional electrocatalyst for highly sensitive sensing. *J. Electroanal. Chem.* **861**, 113945 (2020).
60. Baghayeri, M., Mahdavi, B., Hosseinpor-Mohsen Abadi, Z. & Farhadi, S. Green synthesis of silver nanoparticles using water extract of *Salvia leriifolia*: Antibacterial studies and applications as catalysts in the electrochemical detection of nitrite. *Appl. Organomet. Chem.* **32**(2), e4057 (2018).
61. Maleki, B., Baghayeri, M., Abadi, S. A. J., Tayebee, R. & Khojastehnezhad, A. Ultrasound promoted facile one pot synthesis of highly substituted pyran derivatives catalyzed by silica-coated magnetic $NiFe_2O_4$ nanoparticle-supported H 14 [NaP 5 W 30 O 110] under mild conditions. *RSC Adv.* **6**(99), 96644–96661 (2016).
62. Baghayeri, M., Amiri, A., Alizadeh, Z., Veisi, H. & Hasheminejad, E. Non-enzymatic voltammetric glucose sensor made of ternary NiO/Fe_3O_4-SH/para-amino hippuric acid nanocomposite. *J. Electroanal. Chem.* **810**, 69–77 (2018).
63. Baghayeri, M., Maleki, B. & Zarghani, R. Voltammetric behavior of tiopronin on carbon paste electrode modified with nanocrystalline $Fe_{50}Ni_{50}$ alloys. *Mater. Sci. Eng. C* **44**, 175–182 (2014).
64. Sadeghi, R., Karimi-Maleh, H., Bahari, A. & Taghavi, M. A novel biosensor based on ZnO nanoparticle/1, 3-dipropylimidazolium bromide ionic liquid-modified carbon paste electrode for square-wave voltammetric determination of epinephrine. *Phys. Chem. Liq.* **51**(6), 704–714 (2013).
65. Alavi-Tabari, S. A., Khalilzadeh, M. A. & Karimi-Maleh, H. Simultaneous determination of doxorubicin and dasatinib as two breast anticancer drugs uses an amplified sensor with ionic liquid and ZnO nanoparticle. *J. Electroanal. Chem.* **811**, 84–88 (2018).
66. Yuan, B. *et al.* Graphene oxide/nickel oxide modified glassy carbon electrode for supercapacitor and nonenzymatic glucose sensor. *Electrochim. Acta* **88**, 708–712 (2013).
67. A. Dehdashti, A. Babaei, Highly sensitive electrochemical sensor based on Pt doped NiO nanoparticles/MWCNTs nanocomposite modified electrode for simultaneous sensing of piroxicam and amlodipine. Electroanalysis.
68. V. Arabali, S. Malekmohammadi, F. Karimi, Surface amplification of pencil graphite electrode using CuO nanoparticle/polypyrrole nanocomposite; A powerful electrochemical strategy for determination of tramadol. Microchem. J. 105179 (2020).
69. Hojjati-Najafabadi, A. *et al.* Determination of tert-butylhydroquinone using a nanostructured sensor based on CdO/SWCNTs and ionic liquid. *Int. J. Electrochem. Sci* **15**, 6969–6980 (2020).
70. H. Karimi-Maleh, F. Karimi, S. Malekmohammadi, N. Zakariae, R. Esmaeili, S. Rostamnia, M.L. Yola, N. Atar, S. Movagharnezhad, S. Rajendran, An amplified voltammetric sensor based on platinum nanoparticle/polyoxometalate/two-dimensional hexagonal boron nitride nanosheets composite and ionic liquid for determination of *N*-hydroxysuccinimide in water samples. *J. Mol. Liq.* (2020).

Acknowledgements
The authors hereby express their thanks for the support rendered by Nanjing Forestry University (Grant nos. 163020139 and 163020211), Science and Technology Department of Jiangsu Province (BK2020043008) and National Natural Science Foundation of China (5201101466).

Author contributions
H.K.M., F.K., and F.S. organized all experiments and wrote the manuscript.; Y.O., G.M., A.R., and A.A., performed all experiments. They have also drawn the figures.

Competing interests
The authors declare no competing interests.

Additional information
Correspondence and requests for materials should be addressed to H.K.-M., F.K. or F.S.

Reprints and permissions information is available at www.nature.com/reprints.

Publisher's note Springer Nature remains neutral with regard to jurisdictional claims in published maps and institutional affiliations.